Unit cell of strained GeSi

J. C. Woicik and C. E. Bouldin
National Institute of Standards and Technology, Gaithersburg, Maryland 20899

K. E. Miyano
Department of Physics, Brooklyn College, Brooklyn, New York 11210

C. A. King
Bell Laboratories, Lucent Technologies, Murray Hill, New Jersey 07974

(Received 9 December 1996)

The local structure within the unit cell of strained-GeSi layers grown on Si(001) has been examined by polarization-dependent extended x-ray-absorption fine structure. First-neighbor bond lengths are found to deviate only slightly from their unstrained values; however, the distortion of the cubic-unit cell by strain leads to measurable polarization-dependent changes in first-shell coordination and second-shell distances. A unifying picture of bond lengths and elasticity in strained-layer semiconductors is presented. [S0163-1829(97)03823-X]

When a thin semiconductor film with lattice constant a is grown coherently ($a_{\parallel}=a_s$) on a substrate with a different lattice constant a_s, the layer tetragonally distorts in an attempt to conserve its unit-cell volume. Because real materials are compressible, this distortion is more accurately described by a macroscopic-elastic theory,[1] which, for an isotropic cubic layer grown on a (001) substrate, relates the layer's strain parallel, $\varepsilon_{\parallel}=(a_{\parallel}-a)/a$, and perpendicular, $\varepsilon_{\perp}=(a_{\perp}-a)/a$, to the interface through the elastic constants C_{11} and C_{12} by

$$\varepsilon_{\perp}=-2(C_{12}/C_{11})\varepsilon_{\parallel}. \tag{1}$$

Due to the technological importance of heterojunction devices, it is not surprising that extended x-ray-absorption fine structure (EXAFS) has been used to study the local structure of strained-semiconductor layers in detail; however, what is surprising is that—despite the consensus that bond lengths have a strong tendency to remain close to their natural values—numerous conflicting reports on the microscopic-strain status have been put forward. In some cases, the strain has been found to have remarkable effects on bond lengths,[2,3] while others have found little or no effect.[4–8] Others yet have reported the counterintuitive result that bonds actually elongate in layers under compression.[9]

In order to resolve the issue of bond-length strain, we have performed high-resolution polarization-dependent extended x-ray-absorption fine-structure measurements on strained and well characterized Ge_xSi_{1-x} ($x=0.216$ and 0.219) layers grown on Si(001). Only by performing a relative polarization-dependent measurement can the effects of strain be isolated.

The samples studied were from a group of strained Ge_xSi_{1-x} heterojunction-bipolar transistors grown on Si(001). Details of the sample preparation and characterization have been reported previously.[10] The perpendicular lattice constants of the two films studied were $a_{\perp}=5.5116\pm0.002$ Å and 5.5106 ± 0.002 Å, as determined by x-ray diffraction. Because the lattice constant of an unstrained GeSi film of similar composition is 5.476 Å,[11] this 0.035-Å expansion of the perpendicular lattice constant corresponds to a strain $\varepsilon_{\perp}=0.64\pm0.04$ %, in complete agreement with the prediction of Eq. (1) ($\varepsilon_{\perp}=0.64$). Our diffraction results therefore confirm that both films are macroscopically strained to match the in-plane lattice constant of the silicon substrate.

Before we discuss our polarization-dependent data, it is useful to quantify the bond lengths within the strained-GeSi layers. Figure 1(a) shows the k^2-weighted Ge K-edge EXAFS from the $x=0.219$ Ge_xSi_{1-x} layer and its Fourier-filtered first-shell contribution. Figure 1(b) shows the best fit to the Fourier-filtered signal assuming both Ge and Si first-shell backscattering. These components are closely represented by the experimentally determined EXAFS from crystalline Ge and GaP, which have known structures. The bond lengths determined from the fit are $r_{\text{Ge-Ge}}=2.43\pm0.02$ Å and $r_{\text{Ge-Si}}=2.38\pm0.02$ Å; they lie within the experimental error to the bond lengths determined in both amorphous[12] and crystalline[13–16] Ge_xSi_{1-x} alloys over the entire composition range. In particular, the Ge-Ge bond length is close to the bond length in crystalline Ge (2.45 Å), but it deviates significantly from the bond length in the crystalline Si substrate (2.35 Å). Our measurement therefore suggests that the strain within the GeSi layer is accommodated primarily through bond-angle rather than bond-length distortions. Had the bond angles remained fixed at their average tetrahedral values, coherency with the Si substrate would produce a cubic rather than a tetragonal distortion.

In order to investigate the nature of this distortion further, we turn our attention to the *virtual* tetrahedron shown in Fig. 2. This tetrahedron is under compressive strain in the xy plane, and we may estimate the microscopic effects of strain as follows. The lattice parameters parallel and perpendicular to the interface are given in terms of the bond length r and bond angle θ by

$$a_{\perp}=4r\cos(\theta/2) \quad \text{and} \quad a_{\parallel}=2\sqrt{2}r\sin(\theta/2). \tag{2}$$

0163-1829/97/55(23)/15386(4)/$10.00 © 1997 The American Physical Society

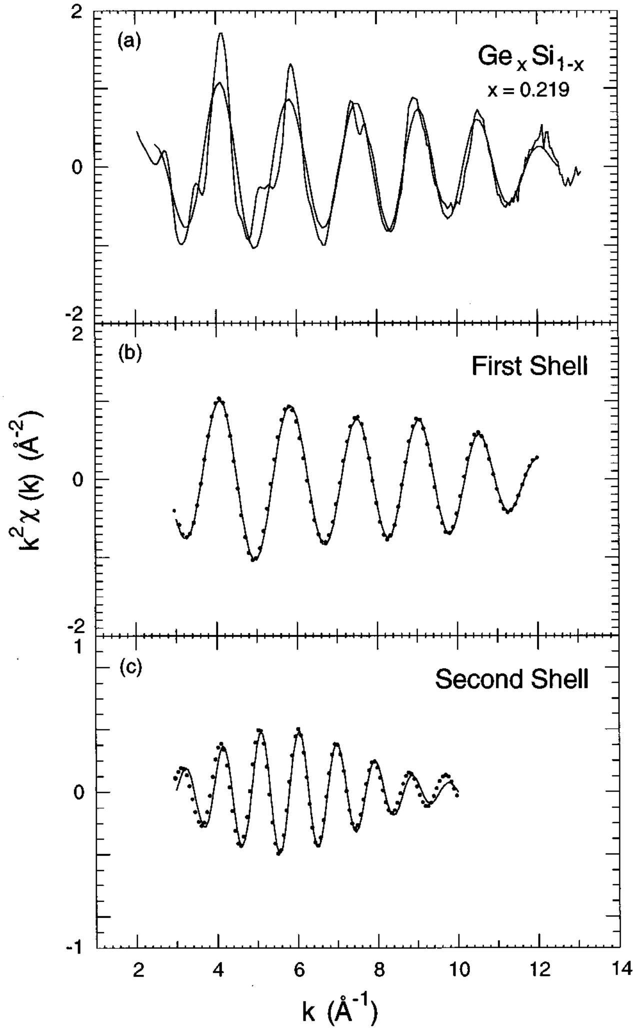

FIG. 1. (a) The k^2-weighted Ge K-edge EXAFS, $k^2\chi(k)$, from the 21.9 at. % Ge, pseudomorphic-Ge_xSi_{1-x} layer on Si(001). Superimposed on the data is the Fourier-filtered first-shell contribution; (b) the fit to the first-shell contribution assuming Ge and Si backscattering. The solid line is the fit, and the dots are the data points of the backtransform. (c) Similar fit for the second-shell contribution.

If we differentiate these equations, to first order we can relate the *macroscopic* strains, $\varepsilon_\perp$ and $\varepsilon_\parallel$, to the *microscopic* distortions Δr, the bond stretch, and $\Delta\theta$, the bond bend:

$$\varepsilon_\perp \equiv \Delta a_\perp / a = (\Delta r/r) - \sqrt{2}/2(\Delta\theta)$$

and

$$\varepsilon_\parallel \equiv \Delta a_\parallel / a = (\Delta r/r) + \sqrt{2}/4(\Delta\theta). \tag{3}$$

Rewriting these equations and defining $\alpha \equiv (\Delta r/r)/(\Delta\theta)$ as the ratio of the bond stretch to bond bend, we arrive at

$$\varepsilon_\perp = -2[(1-\sqrt{2}\alpha)/(1+2\sqrt{2}\alpha)]\varepsilon_\parallel . \tag{4}$$

Using Eq. (1) we can write α in terms of the macroscopic elastic constants C_{11} and C_{12}:

$$\alpha = \sqrt{2}/2[(1-C_{12}/C_{11})/(1+2C_{12}/C_{11})], \tag{5}$$

which is the microscopic analog to Eq. (1). The elastic constants tabulated by Hornstra and Bartels[1] render $\alpha = 0.25$ for an alloy of this composition, confirming the rigid-bond model. Note that Eq. (4) reproduces the conservation of volume, $\varepsilon_\perp = -2\varepsilon_\parallel$, when $\alpha \to 0$. Implicit in the above formulas is the presence of a finite bond-length compression. This is clear because the ratio C_{12}/C_{11} is less than 1 for all of the typical semiconductors.[1]

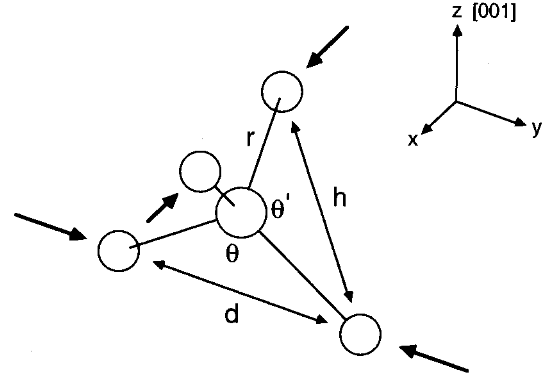

FIG. 2. A tetrahedron under biaxial compression in the xy plane with equivalent first-neighbor bond lengths r. Here $z = \mathbf{n}$ is the [001] direction. The in- and out-of-plane second-neighbor distances are $d = 2r\,\sin(\theta/2)$ and $h = 2r\,\sin(\theta'/2)$.

Because the strained layer is pseudomorphic with the Si substrate, $\Delta a_\parallel$ is known, and the distortions can be calculated. The compression in the first-neighbor bond length is $\Delta r = -0.008$ Å, and the bond angles are shifted anisotropically with respect to the interface: $\Delta\theta = -0.8°$ and $\Delta\theta' = +0.4°$.[17] These distortions translate to an increase in perpendicular lattice constant, $\Delta a_\perp = 0.035$ Å, which is identical to the prediction of Eq. (1).

Although our estimate of a small but finite bond-length compression, 0.008 Å, lies within the typical EXAFS uncertainty for this binary-alloy system, it may explain why our bond lengths fall on the smaller side of the bond lengths recently reported for unstrained-crystalline GeSi alloys.[16] In this work, a small compositional dependence of the bond lengths was reported.

Because the small strain-induced bond-length change is negative, the distortion of the tetrahedral angles must account for the much larger, 0.035 Å, expansion in $a_\perp$. This relatively large distortion should be evident in a second-shell EXAFS analysis. Unfortunately, errors in second-neighbor distances are typically of this order. Nonetheless, Fig. 1(c) shows a fit to the second-shell EXAFS once again assuming Ge and Si backscattering. We have modeled the Ge backscattering by the second-shell EXAFS from crystalline Ge, and the Si backscattering by the second-shell EXAFS from an As-implanted, laser-annealed Si wafer.[18] The second-neighbor distances determined from this fit are $r_{\text{Ge-Ge}} = 3.84 \pm 0.04$ Å and $r_{\text{Ge-Si}} = 3.83 \pm 0.04$ Å. Because the second-neighbor distance in crystalline Si is 3.84 Å, it is clear that, while first-neighbor bond lengths are found to deviate only slightly from their natural values, EXAFS-averaged second-neighbor distances follow more closely a virtual-crystal description. (The second-neighbor distance in crystalline Ge is 4.00 Å.) Similar results have been found for the pseudobinary-$In_xGa_{1-x}As$ alloy system.[19]

We now turn to our polarization-dependent data. Figure 3

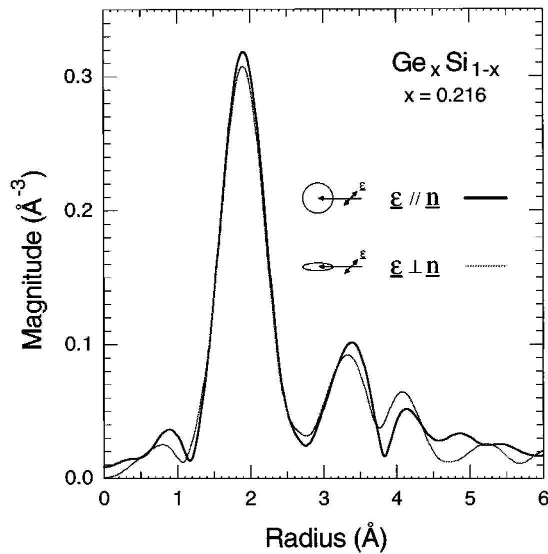

FIG. 3. The Fourier transforms of the k^2-weighted Ge K-edge EXAFS from the 21.6 at. % Ge layer recorded with the polarization vector of the synchrotron radiation aligned parallel ($\boldsymbol{\varepsilon}\|\mathbf{n}$) and perpendicular ($\boldsymbol{\varepsilon}\perp\mathbf{n}$) to the surface normal. These transforms were calculated with a Gaussian window.

shows the Fourier transforms of the k^2-weighted Ge K-edge EXAFS from the $x=0.216$ sample recorded with the polarization vector of the synchrotron radiation aligned parallel ($\boldsymbol{\varepsilon}\|\mathbf{n}$) and perpendicular ($\boldsymbol{\varepsilon}\perp\mathbf{n}$) to the surface normal. Due to the $|\boldsymbol{\varepsilon}\cdot\mathbf{r}|^2$ dependence of the EXAFS equation, these data preferentially sample bonds which are oriented either perpendicular or parallel to the interface. These data therefore constitute a relative measurement, and their relative accuracy is much improved over the absolute bond-length determinations of Fig. 1. Significant differences exist between the two data sets in both the first and second shells. Most notably, the amplitude of both shells is reduced at the normal polarization, and the position of the second shell is shifted towards smaller radii. These effects are observed in the filtered data, which we have plotted in Fig. 4. Note that, while no phase difference is detected in the first shell, a large polarization-dependent phase difference is present in the second shell. Concomitant with this phase difference is a damping of the second-shell data recorded at the normal polarization.

If we use the data recorded in the parallel geometry to model the data recorded in the normal geometry, the following relative changes in bond length and amplitude of the first coordination shell are obtained: $\Delta r_1=-0.001\pm0.005$ Å, and $\Delta N_1/N_1\sim-5\%$. The corresponding relative changes in the second-shell distance and damping are $\Delta r_2=-0.02\pm0.01$ Å and $\Delta\sigma_2^2\sim3\times10^{-3}$ Å^2.

We are now in a position to interpret these relative changes within the context of our microscopic model. Because we have calculated both Δr and $\Delta\theta$, we can also calculate d, the second-neighbor distance parallel to the interface, and h, the second-neighbor distance perpendicular to the interface. Due to the strain-induced tetragonal distortion, these distances should deviate from the single averaged distance for an unstrained-GeSi layer of this composition, 3.872 Å. Using $d=2r\,\sin(\theta/2)$ and $h=2r\,\sin(\theta'/2)$, the results are

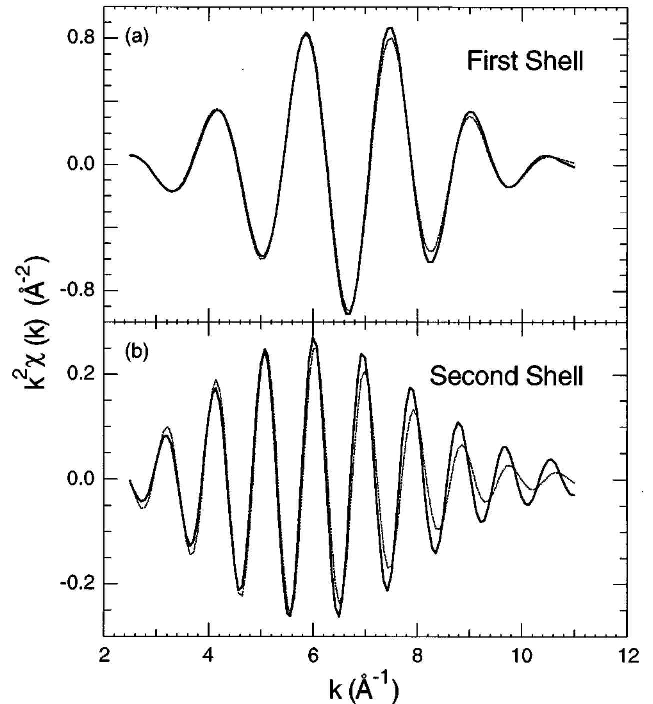

FIG. 4. (a) First-shell Fourier-filtered data from Fig. 3. (b) Similar second-shell data.

$d=3.840$ Å (identical to the Si substrate) and $h=3.868$ Å. This bimodal distribution of averaged second-neighbor distances is a direct result of the strain-induced anisotropic shifts of bond angles relative to the interface. It also accounts, in part, for the static contribution to the damping of the second-shell data recorded at normal incidence.[20]

Because first-neighbor bond lengths show no polarization dependence, the relative change in second-neighbor distances is a direct confirmation of the relative change in bond angles, which in turn will also affect the polarization-dependent relative coordination numbers. For example, $N_\perp$, the first-shell coordination perpendicular to the interface is proportional to $4\cos^2(\theta/2)$, while $N_\|$ is proportional to $2\sin^2(\theta/2)$. Consequently, $\Delta N_1/N_1$ is calculated to be -3%. On the other hand, because all four first-neighbor bonds of our virtual tetrahedron have the same orientation with respect to the interface, Δr is equal for all four bonds, and Δr_1, the relative difference, should be identically equal to zero from symmetry. Both predictions fall within our experimental uncertainty.

Due to the tetrahedral geometry, each atom has four in-plane second-neighbors, d, and eight out-of-plane second neighbors, h. Because d lies within the plane of the interface, but h has a component perpendicular to it, the $\boldsymbol{\varepsilon}\|\mathbf{n}$ measurement will yield $d=h$; the $\boldsymbol{\varepsilon}\perp\mathbf{n}$ measurement will yield $d=1/2(h+d)$. Hence, $\Delta r_2=1/2(d-h)=-0.014$ Å, in agreement with what is experimentally observed. However, using $\Delta\sigma_2^2\sim1/4(d-h)^2=2\times10^{-4}$ Å^2 underestimates $\Delta\sigma_2^2$ significantly. This finding may be reconciled with an asymmetric strain-induced distribution of second-neighbor distances within the compressed plane of the interface that is absent in the normal relaxed direction,[21] i.e., a much larger and assymmetric distribution is found in θ rela-

tive to θ'. Despite this one discrepancy, all other observations are in accord with our microscopic model.

In conclusion, we have performed a detailed microscopic study of the local structure of strained-GeSi layers grown on Si(001). Although strain does not notably alter the first-shell bond lengths to within our EXAFS detectability limit, bond-angle distortions are found to affect first-shell coordination and second-shell distances. These distortions have been explained by a simple microscopic model derived from macroscopic-elastic theory. We feel that our results are of general consequence to all strained-layer semiconductor systems.

This work was performed on beamline X23-A2 of the National Institute of Standards and Technology at the National Synchrotron Light Source at Brookhaven National Laboratory. The National Synchrotron Light Source is supported by the U.S. Department of Energy.

[1] J. Hornstra and W. J. Bartels, J. Cryst. Growth **44**, 513 (1978).

[2] M. G. Proietti, F. Martelli, S. Turchini, L. Alagna, M. R. Bruni, T. Prosperi, M. G. Simeone, and J. Garcia, J. Cryst. Growth **127**, 592 (1993).

[3] H. Oyanagi, Y. Takeda, T. Matsushita, T. Ishiguro, T. Yao, and A. Sasaki, Superlatt. Microstruct. **4**, 413 (1988).

[4] J. C. Woicik, C. E. Bouldin, M. I. Bell, J. O. Cross, D. J. Tweet, B. D. Swanson, T. M. Zhang, L. B. Sorensen, C. A. King, J. L. Hoyt, P. Pianetta, and J. F. Gibbons, Phys. Rev. B **43**, 2419 (1991).

[5] M. Matsuura, J. M. Tonnerre, and G. S. Cargill III, Phys. Rev. B **44**, 3842 (1991).

[6] E. Canova, A. I. Goldman, S. C. Woronick, Y. H. Kao, and L. L. Chang, Phys. Rev. B **31**, 8308 (1985).

[7] M. G. Proietti, S. Turchini, J. Garcia, G. Lamble, F. Martelli, and T. Prosperi, J. Appl. Phys. **78**, 6574 (1995).

[8] C. Lamberti, S. Bordiga, F. Boscherini, S. Pascarelli, G. M. Schiavini, C. Ferrari, L. Lazzarini, and G. Salviati, J. Appl. Phys. Lett. **64**, 1430 (1994).

[9] M. G. Proietti, S. Turchini, J. Garcia, G. Lamble, F. Martelli, and T. Prosperi, J. Appl. Phys. **78**, 6574 (1995).

[10] C. A. King, J. L. Hoyt, and J. F. Gibbons, IEEE Trans. ElectroDevices **ED-36**, 2093 (1989).

[11] J. P. Dismukes, L. Ekstrom, and R. J. Paff, J. Phys. Chem. **68**, 3021 (1964).

[12] L. Incoccia, S. Mobilio, M. G. Proietti, P. Fiorini, C. Giovanella, and F. Evangelisti, Phys. Rev. B **31**, 1028 (1985).

[13] S. Minomura, K. Tsuji, M. Wakagi, T. Ishidate, K. Inoue, and M. Shibuya, J. Non-Cryst. Solids **59&60**, 541 (1983).

[14] H. Kajiyama, S. Muramatsu, T. Shimada, and Y. Nishino, Phys. Rev. B **45**, 14 005 (1992).

[15] D. B. Aldrich, R. J. Nemanich, and D. E. Sayers, Phys. Rev. B **50**, 15 026 (1994).

[16] Jeff Aubry, Master of Engineering thesis, McMaster University, September 1996.

[17] To the first order, $\Delta\theta' = -1/2\Delta\theta$.

[18] A. Erbil, W. Weber, G. S. Cargill III, and R. F. Boehme, Phys. Rev. B **34**, 1392 (1986).

[19] J. C. Mikkelson, Jr. and J. B. Boyce, Phys. Rev. B **28**, 7130 (1983).

[20] $\sin(2kr_1+\phi)+\sin(2kr_2+\phi) = 2\cos(k[r_2-r_1])\sin(k[r_2+r_1]+\phi) \sim 2\exp(-1/2k^2[r_2-r_1]^2)\sin(k[r_2+r_1]+\phi)$.

[21] G. Bunker, Nucl. Instrum. Methods Phys. Res. **207**, 437 (1983).